



Determining cyclic flow curves using the in-plane torsion test

Qing Yin¹, A. Erman Tekkaya (1)*, Heinrich Traphöner

Institut für Umformtechnik und Leichtbau (IUL), Technische Universität Dortmund, 44227 Dortmund, Germany



ARTICLE INFO

Keywords:
Flow stress
Sheet metal
Kinematic hardening

ABSTRACT

A new method of determining cyclic stress–strain curves for characterizing kinematic hardening of sheet materials is introduced utilizing the in-plane torsion test and optical strain measurement. The test enables the simultaneous recording of multiple cyclic stress–strain curves with different amplitudes of plastic strain at load reversal in one single test and with one single specimen. Cyclic flow curves are obtained for DP600, DP800, DX54D, and AA5182, and compared with the Miyauchi shear test. Material parameters for a typical kinematic hardening model are determined. Multiple cyclic stress–strain curves result significantly different model parameters as obtained by a single cyclic curve.

© 2015 CIRP.

1. Introduction

Kinematic hardening behaviour [1] is one main aspect of material modelling for numerical simulation of sheet forming processes and has significant influence on the prediction of spring-back. This behaviour is described in commercial finite element software by the Chaboche-Roussilier [2] or Yoshida-Uemori [3] model usually. The parameter identification process for these models requires a mechanical test with the capability of load reversal. For sheet materials, three types of test approaches are known, which is the tension-compression test [4], the cyclic planar shear test [5], and the cyclic bending test [6]. These tests show some disadvantages: the buckling tendency during compression [7], the inhomogeneity in the edges of the shear zones [8] and the unavailability of stress-strain data in bending tests. Approaches to prevent buckling of sheet samples in tension-compression tests are presented using supporting devices [9] or optimized specimen geometries [10]. High experimental effort, friction, and deviation from the uniform uniaxial stress state can become disadvantageous. To discover the various effects of kinematic hardening, a cyclic flow curve with at least one load reversal and sufficient plastic deformation in both directions is required: The Bauschinger-effect describes the reduction of the yield stress after load reversal [11] and is visible in the cyclic stress–strain curves of many steel and aluminium alloys. Depending on the material, a smooth transition after the elastic unloading (e.g. for dual phase steels) or work-hardening stagnation leading to a temporarily flat flow curve may be observed as further effects. Due to the high experimental effort, the parameter identification is normally performed on the basis of one loading-reloading path, while little is known about the dependence of these kinematic hardening effects from the pre-straining.

In the present work, a novel experimental approach is developed using the in-plane torsion test and optical strain

measurement by digital image correlation. This method is capable of simultaneously determining a large number (about 50) of cyclic flow curves with different pre-strain levels using a single specimen and a single test run. It is also shown that the utilization of a large number of cyclic curves effects the parameter values of the kinematic hardening models significantly.

2. The in-plane torsion test

The in-plane torsion test was firstly introduced by Marciniak [12] for determining cyclic hardening behaviour of copper. It was then utilized to investigate the formability of metal sheets [13] and for the identification of flow curves [14]. One main advantage of the in-plane torsion test is its capability of determining the flow curve until high equivalent plastic strains of up to 1.0 [15]. Recently, new evaluation methods are developed for this test on the basis of optical strain measurement with digital image correlation [16].

The basics of the in-plane torsion test. The specimen of the in-plane torsion test is a round sheet sample. It is clamped concentrically on the outer rim and in the central area, as shown in Fig. 1. By planar rotation of the outer fixture against the inner ones, the free circular area between the clamps is loaded by planar simple shear.

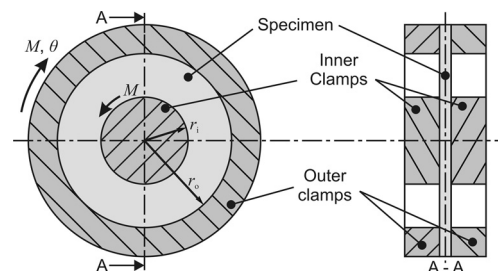


Fig. 1. Schematic design of the in-plane torsion test [14].

* Corresponding author.

E-mail address: erman.tekkaya@iul.tu-dortmund.de (A.E. Tekkaya).

¹ Present address: Volkswagen Osnabrück GmbH, 49084 Osnabrück, Germany.

A major difference to other mechanical tests for flow curve determination is the stress and strain gradient in the specimen. The in-plane shear stress τ at any radial position r is given by

$$\tau = \frac{M}{2\pi \cdot t \cdot r^2} \quad (1)$$

with the currently applied torque M and the sheet thickness t for uniform shear stress in circumferential direction. The highest shear stress is located near the inner clamps, while the stress is decreasing with increasing distance to the rotation centre quadratically. The shear strain γ is defined by

$$\gamma = r \frac{\Delta\theta}{\Delta r} \quad (2)$$

at the radial position r with the rotation angle θ as the slope of the tangent to a material line that was radial before deformation [15]. The shear stress and shear strain can be converted easily to the flow curve using a yield condition. For planar anisotropic materials, an error in the stress calculation will be made with Eq. (1). The measured torque is an integral value over the whole circumference, which does not distinguish the material behaviour in different orientations. For normal anisotropy, the flow stress σ_f and the equivalent plastic strain ε_{eq} is given using the Hill anisotropic yield criterion by

$$\sigma_f = \sqrt{3} \cdot \tau \sqrt{\frac{2(2r_n + 1)}{3(r_n + 1)}}, \quad \varepsilon_{eq} = \frac{\gamma}{\sqrt{3}} \cdot \sqrt{\frac{3(r_n + 1)}{2(2r_n + 1)}} \quad (3)$$

where r_n is the normal anisotropy factor ($r_n = 1$ for isotropy) [17].

One advantage of the in-plane torsion test is the circular closed-loop shear zone which does not have any edges, where notch-effects can cause inhomogeneous stress and strain fields. The achievable strain is either limited by the transferable torque at the inner fixture, by buckling of the specimen, or by a diminishing strain hardening [18].

Simultaneously determining multiple cyclic stress–strain curves. The idea of the present work is to utilize the given gradient of stress and strain on a loaded in-plane torsion specimen to obtain several flow curves simultaneously. As schematically shown in Fig. 2, the strain measurements are performed on locations of different radii with the simultaneous strain measurement method introduced in [19]. When the forward shear loading is applied, the determined stress–strain curves at different radii will be the same having only different ranges. After a certain relative twist of the clamps, several monotonic flow curves (respectively shear strain–shear stress curves) are recorded with different strain ranges. At this state, a load reversal causes each location to unload and reload from its current state. Therefore, an array of cyclic stress–strain curves is created with different pre-strain levels. The longest curve with the highest strain and stress values envelops all other curves and is measured at the smallest radius.

The advantage of this approach is obvious, as it allows obtaining a high amount of information on cyclic hardening behaviour of sheet materials with a high accuracy and small effort in time and cost since a single test is performed. From one specimen only, a set of cyclic

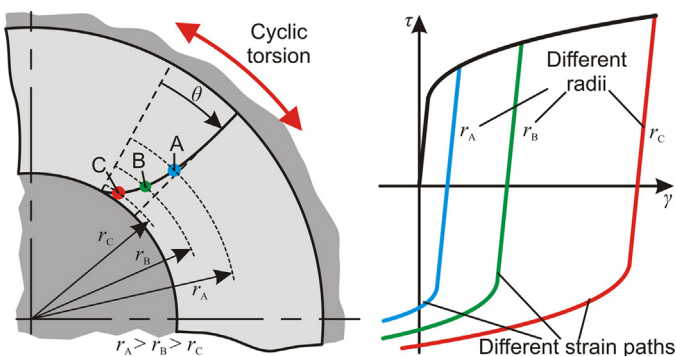


Fig. 2. Approach to simultaneously determine multiple cyclic flow curves using one single in-plane torsion test.

flow curves can be measured with different pre-straining, providing an extensive basis for subsequent parameter identification.

Experimental set-up. The originally designed in-plane torsion device can be placed in a standard uniaxial testing machine [19]. The twisting angle is measured by an incremental rotary encoder with a resolution of 0.016° . Tools are used with an inner clamping radius of $r_i = 15$ mm and an outer clamping radius of $r_o = 30$ mm (Fig. 1). The inner clamping force is set to 50 kN and a rotation speed of ca. $0.05^\circ/\text{s}$ was applied. The optical strain measurement system GOM ARAMIS 5 M utilizes cameras which are arranged above the specimen at a distance of ca. 40 mm. A section of ca. 60° of the specimen is captured with a spatial resolution of ca. 0.01 mm. On the specimen surface, a stochastic pattern is applied as required for greyscale correlation. During loading, the measurement is set to one picture every 3 s. In order to obtain robust measurement results, the strain data is not directly obtained from the provided strain calculation at one single point in the measurement. Instead, circular section cuts, concentrically located to the rotation centre, are created in the post-processing of the measurement. In the area of $r = 15.0$ mm to $r = 20.0$ mm, one section cut is created every 0.1 mm. By tracking the averaged rotation angle of each section cut, the local shear strain can be calculated between two measured radii by Eq. (2). Following this approach, a set of 49 cyclic stress–strain curves is obtained from every single specimen.

3. Experimental results

Four sheet materials are analyzed in the current study: DX54D, DP600, DP800, and AA5182-O. The deep drawing steel DX54D had a sheet thickness of $t = 0.8$ mm. Both dual-phase steels and the aluminium alloy were tested in the thickness of $t = 1.0$ mm. The anisotropy values of each sheet are given in Table 1 as obtained in simple tension tests. A correction of the flow stress due to anisotropy as shown in Eq. (3) is not performed in the current study, since the deviation from the isotropic case is less than 5% for all materials.

Table 1
Anisotropy coefficients of the tested sheet materials.

Material	r_0	r_{45}	r_{90}	r_n	Δr
DX54D	2.03	1.58	2.34	1.88	0.61
DP600	0.82	0.77	0.93	0.83	0.11
DP800	0.83	0.85	0.99	0.88	0.05
AA5182-O	0.81	0.67	0.72	0.72	0.09

The measuring and evaluation approach as described in the previous section is applied on all four materials. In Figs. 3–6, the results of one exemplary measurement for each material are shown. For clarity only 12 curves out of 49 are shown in each graph. The monotonic flow curve is compared with standard uniaxial tensile test and the kinematic hardening behaviour with a cyclic shear tests according to the specimen design of Miyauchi.

For DX54D (Fig. 3), the longest curve is unloaded at a true strain of $\varepsilon \approx 0.3$ with the highest pre-strain. The flow curves for all radii follow the same loading path. Compared to the flow curve measured in the uniaxial tensile test, the torsion curves show a slight different slope after starting from the same value of the initial yield stress. This

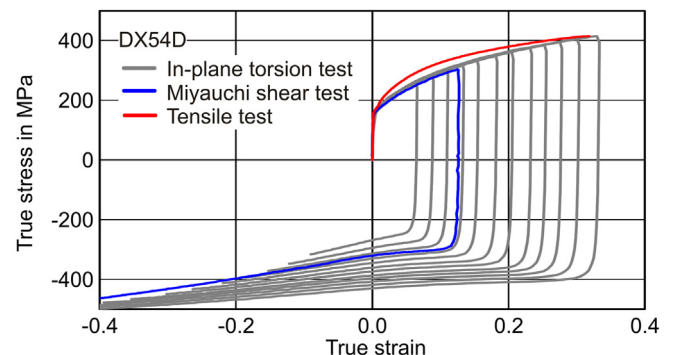


Fig. 3. Set of cyclic flow curves for DX54D in comparison with the result of uniaxial tensile test and a cyclic Miyauchi shear test.

Download English Version:

<https://daneshyari.com/en/article/10673374>

Download Persian Version:

<https://daneshyari.com/article/10673374>

[Daneshyari.com](https://daneshyari.com)